



EUROPEAN  
COMMISSION

Community research



**DELIVERABLE (D-N°:D3:03)**  
**ALC full-scale emplacement experiment**  
**Cell excavation and emplacement report**

Author(s): Jacques Morel, ANDRA (French National Radioactive Waste Management Agency)

Date of issue of this report: 15/09/2013

Start date of project: 01/01/11

Duration: 48 Months

Project co-funded by the European Commission under the Seventh Euratom Framework Programme for Nuclear Research & Training Activities (2007-2011)		
Dissemination Level		
PU	Public	PU
RE	Restricted to a group specified by the partners of the LUCOEX	
CO	Confidential, only for partners of the LUCOEX project	

LUCOEX





## **WP3 - ALC FULL-SCALE EMPLACEMENT EXPERIMENT CELL EXCAVATION AND EMPLACEMENT REPORT**

## CONTENTS

<b>1. Purpose of this document</b>	<b>4</b>
<b>2. Concept and objectives of the experiment</b>	<b>4</b>
<b>2.1 Summary of the concept of high-level waste cells</b>	<b>4</b>
<b>2.2 Experiment strategy</b>	<b>5</b>
2.2.1 Objectives of the "High-level Waste Cells" Programme Unit	5
2.2.2 Feedback from the earlier phases of the "High-level Waste Cells" PU	5
2.2.3 Objectives of phase 3.1 of the "High-level Waste Cells" PU	6
<b>2.3 Specifications for the "heating cell" phase 3.1</b>	<b>6</b>
<b>3. Procedure for "heating cell" phase 3.1</b>	<b>8</b>
<b>3.1 Installation of the peripheral instrumentation</b>	<b>8</b>
3.1.1 Realization of the peripheral boreholes	8
3.1.2 Instrumentation on the GAN access gallery support structures	10
<b>3.2 Cell excavation</b>	<b>10</b>
<b>3.3 Drilling of the last two peripheral boreholes</b>	<b>14</b>
<b>3.4 Installing the liner and insert instrumentation</b>	<b>15</b>
3.4.1 Description of the instrumentation	15
3.4.2 Installation sequence	17
<b>3.5 Installation of the heating elements</b>	<b>18</b>
<b>3.6 Finalisation of the instrumentation of the cell-crossing section</b>	<b>20</b>
<b>4. Initial results</b>	<b>20</b>
<b>4.1 Impact of the cell excavation</b>	<b>20</b>
<b>4.2 Measurements evolution in the cell</b>	<b>23</b>
4.2.1 Liner and insert convergence sensors	23
4.2.2 Convergence sensors on the heating elements	25
4.2.3 Rock/liner clearance reduction sensors	25
4.2.4 Strain gauges	26
4.2.5 Total pressure values	26
4.2.6 Axial extensometer and liner/insert sliding sensors	27
4.2.7 Relative humidity in the cell	27
<b>4.3 Low-power heating test</b>	<b>28</b>
4.3.1 Temperature evolution inside the cell	28
4.3.2 THM impact on the rock mass	28
<b>5. Conclusion</b>	<b>29</b>

## 1. Purpose of this document

This document presents a report on the excavation of heating cell ALC1604 and the installation of its instrumentation. It provides a brief summary of the concept of high-level waste cells and the feedback obtained from the earlier phases of the "High-Level Waste Cells" Programme Unit, together with the objectives of phase 3.1 and its development (excavation and instrumentation). This report also presents the initial results from the excavation work and the low-power heating test carried out between 30 January and 15 February 2013.

## 2. Concept and objectives of the experiment

### 2.1 Summary of the concept of high-level waste cells

According to the reference concept, a high-level waste cell (Figure 1) is a microtunnel of at least 40 metres in length and approximately 0.7 metres in diameter. It comprises a useful section of around 30 metres in length, in which the packages are stored, and a cell head of approximately 10 metres in length. These are positioned favourably in relation to the natural mechanical stress field. The useful section of the cell (the "storage cell"), which houses the packages, has a non-alloy steel liner. The end of the cell is closed by an "end plate", which is also made of non-alloy steel. The cell head is separated from the useful section by a metal radiological protection plug. It has a metal liner<sup>1</sup> (or "insert") containing an assembly made up of a swelling clay plug pressing against a concrete plug, which seals the cell and contributes to safety. This configuration represents the period after the cell has been used and sealed.

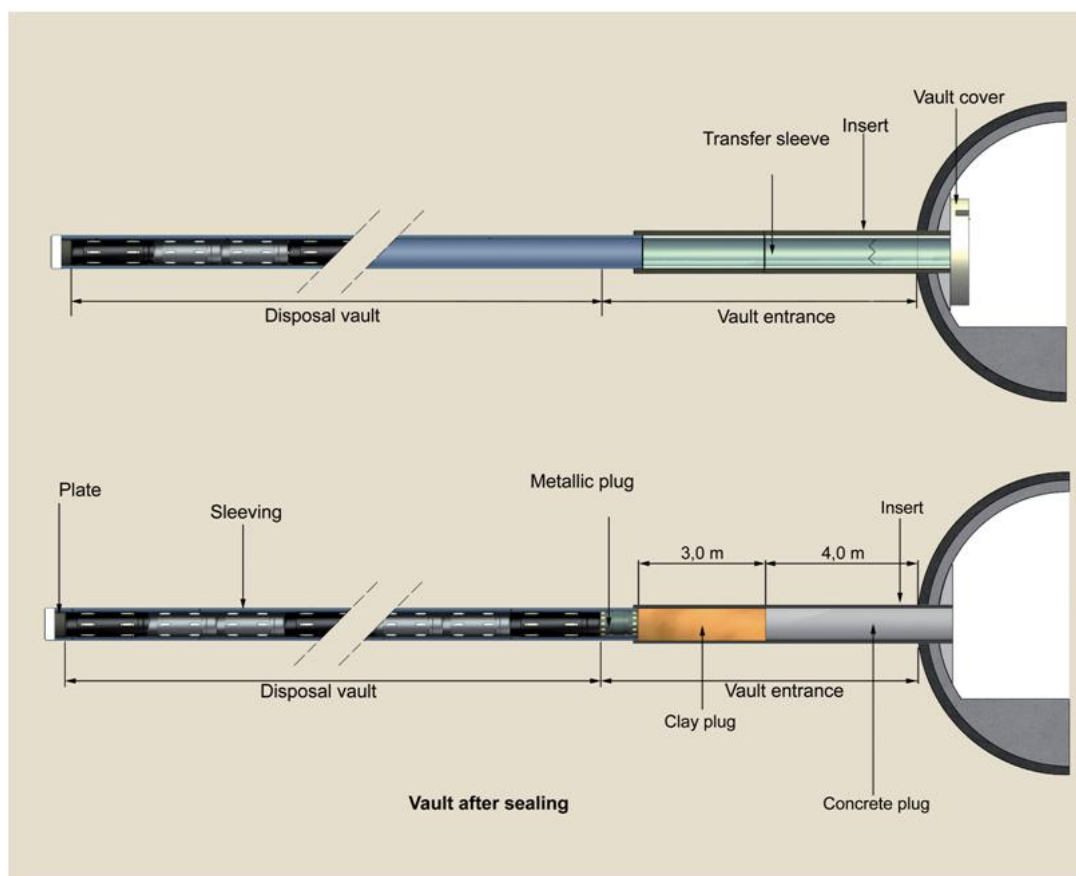


Figure 1 Schematic diagram of a high-level waste cell

<sup>1</sup> The diameter of the liner in the useful section of the cell is smaller than the diameter of the insert in the cell head. This allows it to slide into the insert. The thrust effects associated with its elongation, caused by the rise in temperature due to the exothermic packages, are therefore absorbed without impacting on the cell head assembly.

The useful section of the cell can house around 20 moderately exothermic packages (C0 packages) or six to eight highly exothermic packages. The highly exothermic packages are spaced apart by means of separators to ensure more uniform heat flows. The thickness of the liner, which is around 35 mm at a depth of 560 metres, is determined to maintain the operational clearances needed to remove the stored packages during the reversibility period. The insert in the cell head is also designed to enable the reversible operation of the cell.

## 2.2 Experiment strategy

### 2.2.1 Objectives of the "High-level Waste Cells" Programme Unit

The "High-level Waste Cells" Programme Unit (PU) has two major objectives:

- 1) to check the technological feasibility of cell construction;
- 2) to provide answers to the scientific questions that remain open.

The technological objective involves confirming that it is possible to construct lined cells in the host formation, measuring around 700 mm in diameter and 40 to 80 metres or more in length. The answers that need to be provided particularly relate to the excavation work (the surface condition of the cell walls and the definition of a procedure), the installation of the liner (the annular space that can be reasonably achieved and the method for assembling the sections) and the ability to manage expansion during the heating phase of the storage process (with the operation of a system that slides the liner into the insert in the cell head).

The scientific issues associated with the "High-level Waste Cells" PU relate to managing the thermo-hydro-mechanical (THM) processes that occur on the upper surface of the liner and in the near-field rock (and the typical time frames involved), together with the physico-chemical state of the claystone and the steel of the liner on this upper surface.

#### 2.2.2 Feedback from the earlier phases of the "High-level Waste Cells" PU

During phases 1 and 1b, carried out in 2009 and 2010, the excavation and liner installation methods were tested and a procedure was developed for constructing the cells in the subsequent phases of the Programme Unit. These phases also provided initial data on the hydro-mechanical behaviour of the cells and their environment: the distance of influence around the excavated areas, the mechanical behaviour of the cells and the damage around them.

Phase 2 took place in 2011 and had two objectives:

- to test the construction of a cell head with the installation of an insert;
- to excavate a 40-metre lined cell to study how the clearance between the liner and the claystone would be taken up (by analysing the resaturation kinetics and the load applied on the liner) and its influence on the mechanical behaviour of the liner.

The feedback from the cell head test (cf. Lucoex deliverable D3.1), i.e. jamming of the insert into the ground after 7.5 metres of excavation, was taken into account when specifying the characteristics of the cell head for the "heating cell" phase 3.1. Of particular note, its length was reduced to 6 metres (compared to the 10 metres initially envisaged, as per the reference concept), and the annular space between the insert and the rock was increased from 8 to 12 mm at the radius.

The construction of the 40-metre cell fitted with its equipment allowed us to validate the procedure for installing the instrumentation in the liner, requiring personnel to work inside the cell. Indeed, as the liner was put in place during the course of the excavation work, most of the instrumentation and all of the cables needed to be installed after excavation to avoid any damage to the sensors. The installation of the end plate was also tested and validated at this time.

### 2.2.3 Objectives of phase 3.1 of the "High-level Waste Cells" PU

The goal of phase 3.1 is to study the behaviour of a high-level waste cell under thermal stress, by simulating the release of heat generated by waste packages. The objectives are twofold: to demonstrate the excavation and operation of a high-level waste cell and to understand the THM behaviour of the nearby rock.

The concept of the experiment therefore needs to represent an actual storage cell, to demonstrate the operation of a high-level waste cell for C0 type waste (packages stored without separators) and to enable the study of its impact on the surrounding environment. The main objectives of phase 3.1 are detailed below:

- to excavate a cell, incorporating:
  - the body of the cell, corresponding to the useful section, fitted with a rigid liner;
  - the insert in the cell head;
  - the installation of an end plate at the bottom of the cell;
  - the installation of a plug at the head of the useful section (representing the radiological protection plug);
  - the installation of a closing plate at the head of the insert;
- to study the cell's behaviour under the effect of the thermal load:
  - the mechanical behaviour of the liner and the insert;
  - the operation of the cell head (expansion of the cell body and the process of sliding into the insert);
- to study the impact of the thermal gradient along the cell on the behaviour of the access gallery;
- to analyse the THM behaviour of the rock/liner interface and its impact on the liner's mechanical load (homogeneous or heterogeneous).

This experiment also provides the opportunity to study the THM behaviour of the claystone beyond the interface, principally in terms of the overpressure generated by the heating phase. The data acquired could then be compared to the data from the smaller scale TER and TED thermal experiments, in particular with the digital simulations based on the THM models defined in these experiments.

*NB: The "demonstration test" part, i.e. the demonstration of cell construction and operation in phase 3.1 (like the insert test conducted in phase 2) is part of the European LUCOEX project. The THM analysis of the interface and the near field, which relates more to development research, is not part of the European project.*

## 2.3 Specifications for the "heating cell" phase 3.1

The design choices and the general characteristics of "heating cell" phase 3.1 of the "High-level Waste Cells" experiment are presented in the experiment specifications (cf. Lucoex deliverable D3.2). An overview of the experiment is presented in Figure 2.

The characteristics of cell ALC1604 are as follows:

- a total length of 25 metres, comprising a cell head of 6 metres and a "useful" section of 19 metres, with a 1-metre overlap area between the liner and the insert;
- the excavated cell head measuring 791 mm in diameter, with a fitted insert having an external diameter of 767 mm (providing an annular space of 12 mm at the radius) and a thickness of 21 mm;
- the excavated useful section measuring 750 mm in diameter, with a fitted liner having an external diameter of 700 mm (providing an annular space of 25 mm at the radius) and a thickness of 20 mm;
- an end plate, a plate at the head of the liner and a plate at the head of the insert;
- heat generated over a length of 15 metres at a depth of between 10 and 25 metres.

The instrumentation for the experiment comprises:

- the cell liner instrumentation, with strain gauges, total pressure sensors at the rock/liner interface, rock/liner clearance reduction sensors, relative humidity and temperature sensors in the annular

space between the rock and the liner, an axial extensometer, liner convergence sensors and axial temperature profiles;

- the cell head insert instrumentation, with strain gauges, relative humidity and temperature sensors in the insert, insert convergence sensors and axial temperature profiles;
- the instrumentation in the insert/liner overlap area, with sensors to monitor the liner sliding into the insert;
- five heating elements measuring 3 metres in length with, in addition to the temperature sensors for heat control, sensors to monitor the convergence of the liner and biaxial tiltmeters;
- instrumentation peripheral to the cell, comprising:
  - nine peripheral boreholes made from the GAN access gallery and the perpendicular NRD gallery, fitted with mono- or multi-packers completions, to monitor the interstitial pressure in the rock mass (six boreholes), temperature sensors (two boreholes) and strain sensors (one borehole);
  - instrumentation in the GAN access gallery, comprising:
    - strain gauges on parts of the cell-crossing section;
    - sliding sensors on four arches on each side of the cell;
    - displacement and tilt sensors on the wall of the cell-crossing section;
    - a section (SMR) with radial boreholes equipped with extensometers to measure access gallery deformation;
    - a relative humidity and temperature sensor.

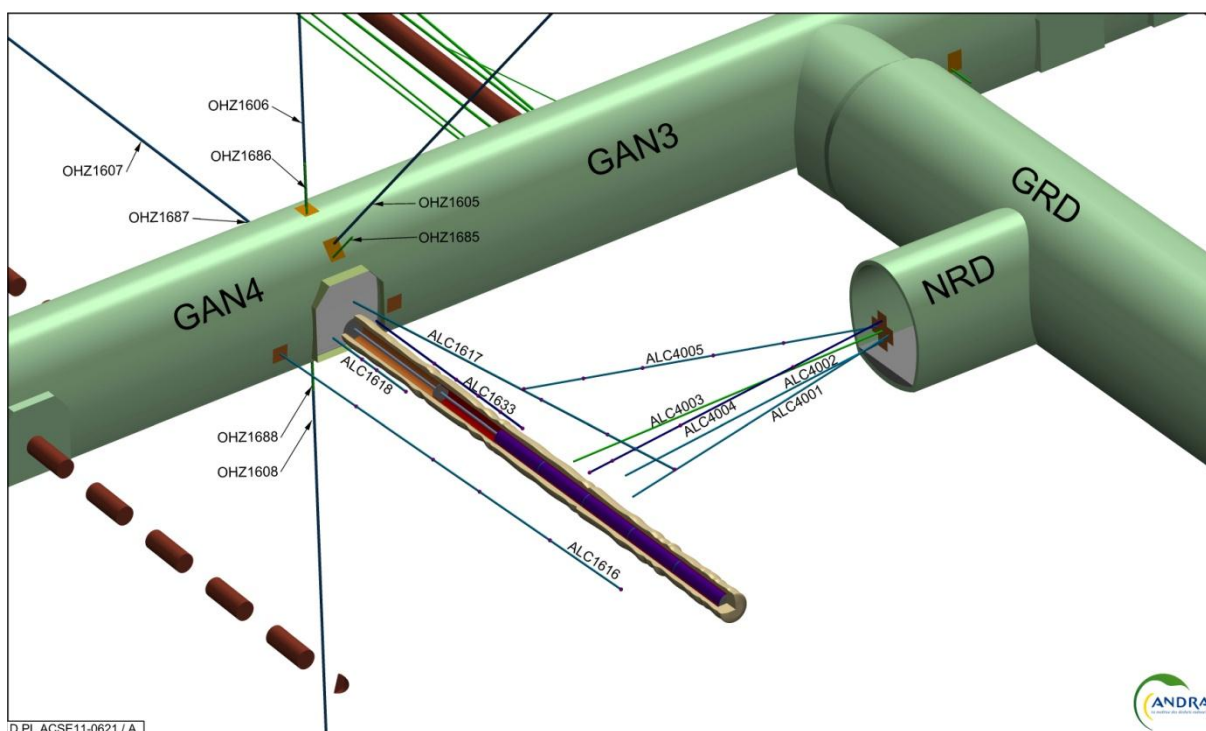


Figure 2 Overview of the "heating cell" experiment

### 3. Procedure for "heating cell" phase 3.1

This section presents the sequence of operations for the "heating cell" experiment in chronological order.

#### 3.1 Installation of the peripheral instrumentation

Most of the boreholes around the cell, as well as some of the instrumentation in the GAN access gallery, were installed prior to the cell excavation to measure its impact on the host rock.

##### 3.1.1 Realization of the peripheral boreholes

Table 1 provides a list of the peripheral boreholes realized before the cell was excavated, together with the date on which they were drilled and their equipment. Most of these boreholes (with the exception of ALC4004) were drilled and fitted with their equipment around a year before the cell was excavated.

*Table 1 Drilling dates for the boreholes made around the heating cell*

Borehole	Gallery	Equipment	Drilling dates
OHZ1605 to 1608	GAN	Extensometers 7 points - SMR	17 to 26/10/2011
OHZ1685 to 1688	GAN	Extensometers 1 point - SMR	14 to 21/10/2011
ALC4001	NRD	Mono-packer completion	3 to 4/11/2011
ALC4002	NRD	Mono-packer completion	2 to 8/11/2011
ALC4003	NRD	Temperature 5 points	26 to 27/10/2011
ALC4004	NRD	Mag-X extensometer 20 points	22 to 23/05/2012
ALC4005	NRD	Multi-packer completion 5 chambers	27/10 to 4/11/2011
ALC1616	GAN	Multi-packer completion 5 chambers	4 to 17/11/2011
ALC1617	GAN	Multi-packer completion 3 chambers	7 to 17/11/2011

The characteristics of these boreholes, together with the actual positions of the measuring points in relation to the cell's axis (taking into account its actual trajectory and the boreholes), are provided in Table 2.



*Table 2 Characteristics of the boreholes and positions of the measuring points*

Borehole	Type of measurement	Length (m)	Ø (mm)	Depth of measuring points in borehole (m)	Radial position / axis of cell (m)	Position at z / axis of cell (m)
ALC4001	Interstitial pressure/T°	12.98	38	12.98	-1.47	-0.27
ALC4002	Interstitial pressure/T°	12.31	38	12.31	-1.94	-0.02
ALC4003	T°	12.86	56	12.86/12/11/ 9/4	-1.06/-1.98/-2.98/ -4.98/-9.98	0.54/0.35/0.27/ 0.23/0.2
ALC4004	Micro-strain	13.10	76	12.8/12.5/12.2/ 11.8/11.3/10.8/ 10.3/9.8/9.3 8.8/8.3/7.8/ 6.8/5.8/4.8/ 3.8/2.8/2.3/ 1.8/1.3	-1.24/-1.54/-1.84/ -2.24/-2.74/-3.24/ -3.74/-4.24/-4.74/ -5.24/-5.74/-6.24/ -7.24/-8.24/-9.24/ -10.24/-11.24/-11.74/ -12.24/-12.74	-0.02/-0.01/0/ 0.01/0.03/0.04/ 0.06/0.07/0.09/ 0.11/0.12/0.14/ 0.17/0.2/0.24/ 0.27/0.3/0.32/ 0.33/0.35
ALC4005	Interstitial pressure/T°	15.00	76	4/7/10/ 12.5/15	-10.13/-7.18/-4.24/ -1.79/0.57	1.14/1.72/2.3/ 2.79/3.27
ALC1616	Interstitial pressure/T°	22.10	76	5/10/13/ 17.5/22	2.78/2.64/2.55/ 2.42/2.3	0.1/0.13/0.14/ 0.22/0.32
ALC1617	Interstitial pressure/T°	22.10	76	13/17.5/22	-0.43/-0.57/-0.72	2.54/3.17/3.84

The locations of the interstitial pressure measurement chambers, the Mag-X extensometer measuring points and the temperature borehole in relation to the cell on a perpendicular plane, are mapped in Figure 3.

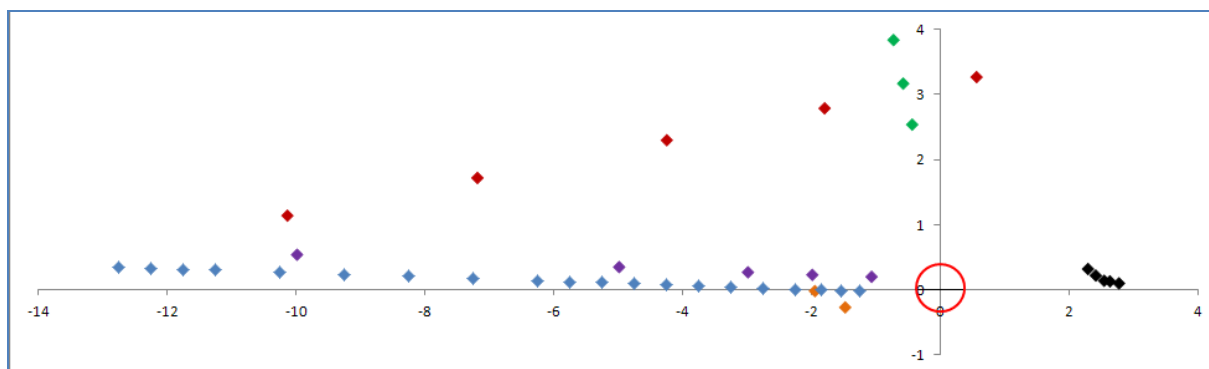


**Figure 3** Distance (in m) of the interstitial pressure, temperature and Mag-X extensometer measuring points in relation to the cell (red circle) – ALC4005 (red), ALC1616 (black), ALC1617 (green), ALC4001 and 4002 (orange), Mag-X (blue), temperature (purple)

### 3.1.2 Instrumentation on the GAN access gallery support structures

Two types of equipment were installed on the support structures in the GAN access gallery:

- 16 strain gauges on the side walls and the crown of the cell-crossing section;
- 8 sensors for monitoring the sliding movements, by the locks on four arches (two on each side of the cell).

These sensors were installed between 10 and 12 October 2012, two weeks before the cell excavation work began.

## 3.2 Cell excavation

The excavation of the cell began on 23 October 2012.

The cell head was excavated from 23 October at 11am to 24 October at 3am, thus taking 16 hours to cover a length of 6 metres (just over 5.5 metres in the ground, equal to 0.35 metres per hour). However, it should be noted that the tip of the cutting head broke at the very end of the borehole. The thrust exerted on the inserts and the drill head remained limited (Figure 5).

The configurations of the drilling machine and the drilling bench were then modified to take account of the change in the diameter of the borehole and the liners (the rock mass had been excavated some tens of centimetres beyond the insert to allow for the deployment of eccentrics 750 mm in diameter). Guide rails were also installed in the inserts so that the liners and the inserts would be concentric. These operations took 11 hours.

The useful section of the cell was excavated in two phases:

- an initial phase from 24 October at 2pm to 26 October at 6am, with excavation up to metric point 24.3, equal to just over 18 metres in 40 hours (0.46 metres per hour); the thrust remained low, even though an increasing rise in pressure was observed on the liners (Figure 6); at 70 cm from the target depth (25 metres), the eccentrics became blocked in the liner at the head, causing the coupling between the conical screw and auger no. 1 to break; as the drill head could not then be pulled out with the drill string, a system of metal chains, requiring intervention by personnel inside the cell, had to be used to release and retrieve it;
- after the machine was repaired, further work by personnel inside the cell, to perforate the face with a pneumatic drill and clear the space required to deploy the eccentrics, failed to allow the drilling work to resume (due to insufficient space between the face and the liner at the head); it was therefore decided to excavate the last few dozen metres by reverse rotation, with a diameter of 600 mm, and then to push the liner sleeve; this procedure was used to excavate an additional 50 cm on 31 October, reaching a depth of around 24.8 metres.

Figure 4 presents several photographs showing different phases of cell excavation.



Drilling station in gallery



Drill head in position



View of the inserts with guide rails



Fixation of the insert at the cell head



Excavation of the useful section

Figure 4

Cell excavation

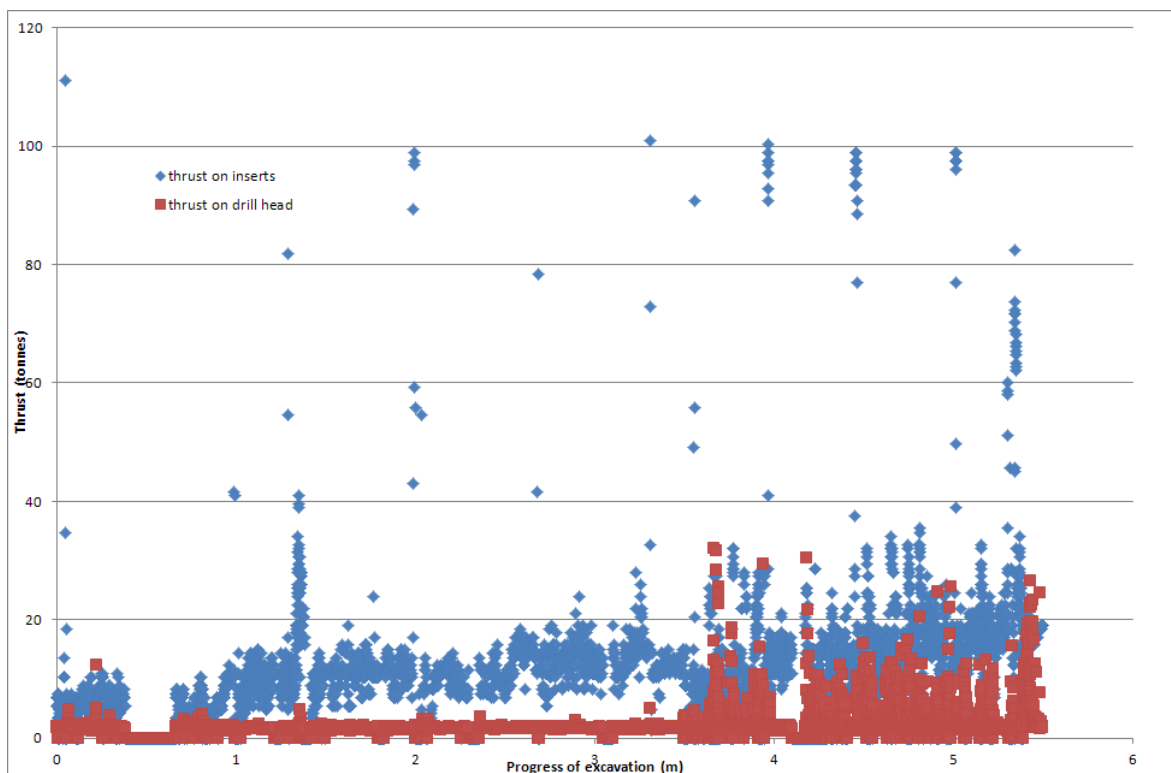


Figure 5 Thrust on the liners and the drill head while excavating the insert

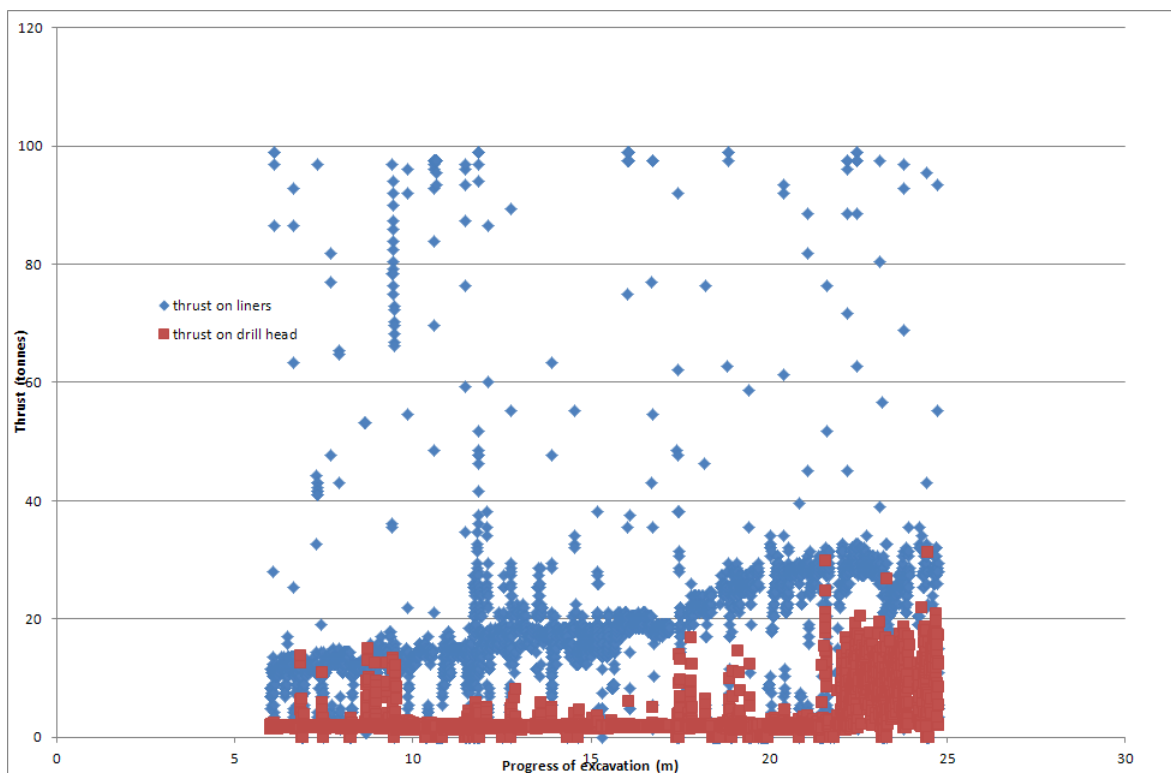
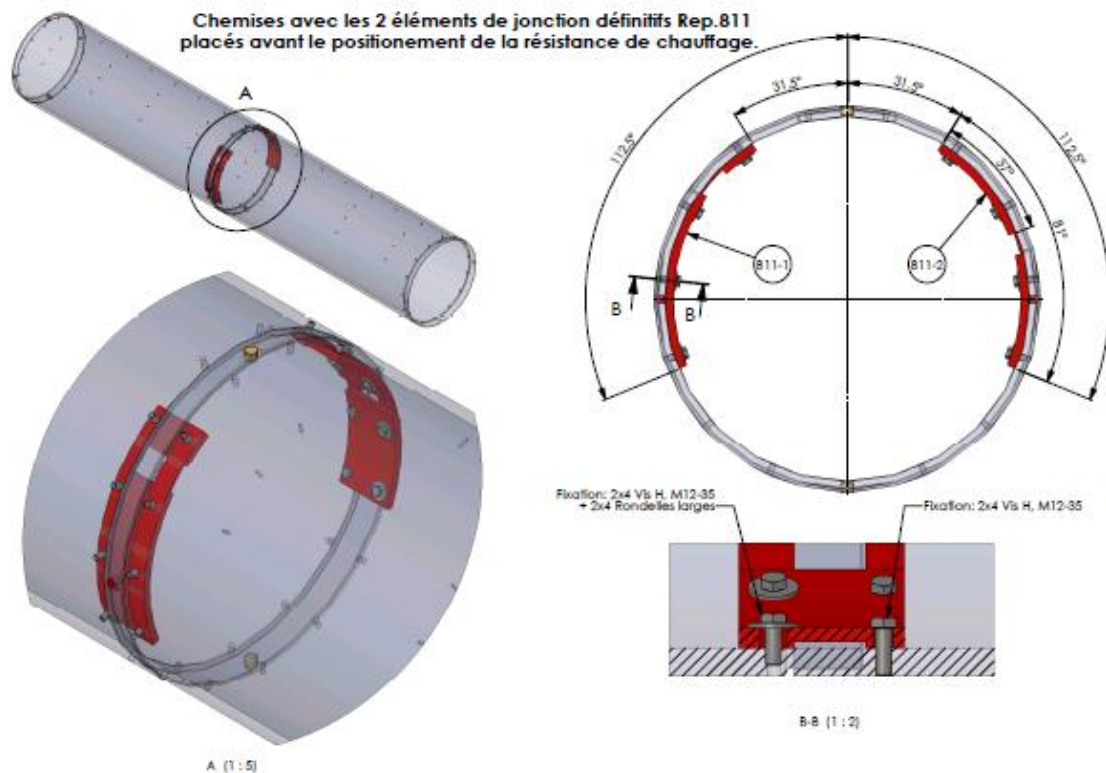


Figure 6 Stress on the liners and the drill head while excavating the useful section

After the cell had been excavated and the machine finally removed, the end plate (Figure 7) and the rigid inter-liner connectors (Figure 8, to ensure liner rigidity as the 2 m long liner sections were socketed to each other) were installed by personnel working inside the cell on 6 and 7 November 2012.



**Figure 7** View of the installed end plate - the reserve openings in liner no. 2 for the gauges and clearance reduction sensors can also be seen here



**Figure 8** Configuration of the rigid inter-liner connectors

A 3D scan of the cell on 6 November, just before the end plate was installed, showed a maximum deviation of 1.6 cm in the horizontal plane and 8.1 cm in the vertical plane (Figure 9). The final bearing was N154.98°E and the overall gradient was 0.24%.



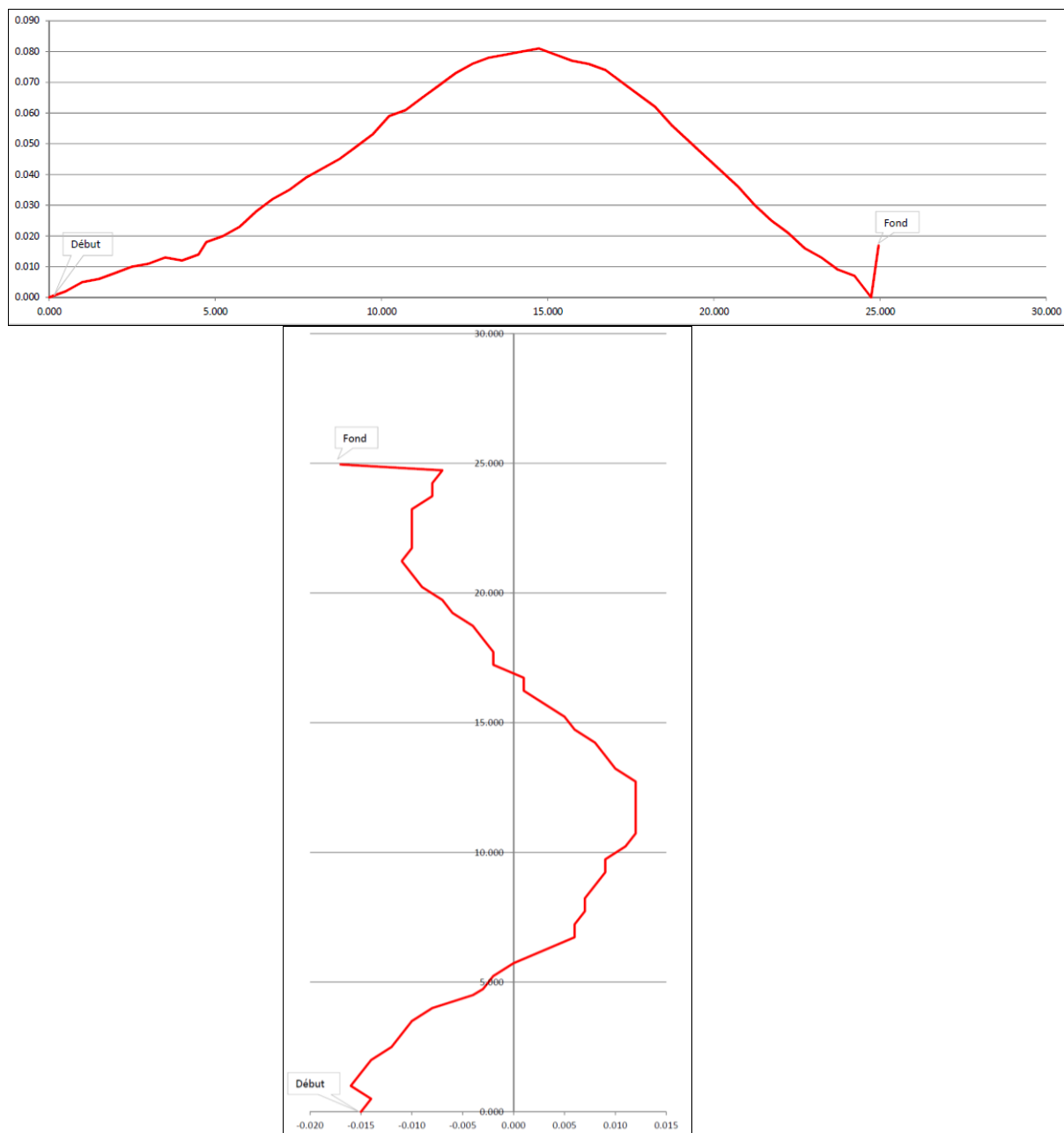


Figure 9 Deviation in the vertical (up) and horizontal (down) planes

### 3.3 Drilling of the last two peripheral boreholes

The last two boreholes, ALC1618 (pore pressure) and ALC1633 (temperature), positioned in parallel to one another on each side of the cell in the horizontal plane (Figure 2), were drilled in the GAN gallery between 12 and 14 November 2012. As these boreholes were located only 50 cm from the cell's wall, drilling them prior to excavation posed too great a risk.

Table 3 summarises the characteristics of these boreholes and the actual positions of the measuring points in relation to the cell's axis (taking its actual trajectory and the boreholes into account).

**Table 3** *Characteristics of the boreholes and positions of the measuring points*

Borehole	Type of measurement	Length (m)	Ø (mm)	Depth of measuring points in borehole (m)	Radial position / axis of cell (m)	Position at z / axis of cell (m)
ALC1618	Interstitial pressure/T°	5.79	76	5/3/2	0.88/0.88/0.87	0.08/0.05/0.03
ALC1633	T°	10.68	76	10/8.5/7/ 5.5/4	-0.9/-0.9/-0.89/ -0.87/-0.86	0.08/0.07/0.06/ 0.06/0.04

### 3.4 Installing the liner and insert instrumentation

Work began to install the liner and insert instrumentation on 19 November 2012. Between 7 and 9 November, Aitemin had worked on site to lay the guide rails for the heating elements. These rails were used by Egis Géotechnique to move the works trolley inside the cell.

#### 3.4.1 Description of the instrumentation

Figure 10 shows the locations of the liner and insert sections fitted with instrumentation in the cell.

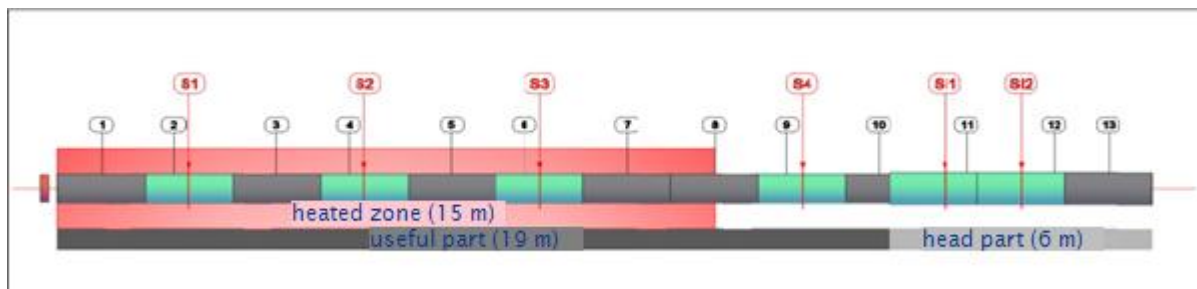


**Figure 10** *Locations of the liner and insert sections fitted with instrumentation*

Each equipped section of liner includes (Figure 11):

- six sectors of strain gauges on the under surface of the liner, with an axial gauge and an orthoradial gauge for each sector; these sectors are positioned horizontally and at 45°; the gauges are attached directly to the steel (Figure 12); they adhere to the bottom of the spot facing, which is 7 mm deep;
- two sectors for measuring the total pressure at the rock/liner interface, positioned at 45°; each total pressure cell consists of three force sensors placed between two steel plates (Figure 13), used to take measurements from which the total pressure is deduced;
- three sectors of sensors for monitoring how the rock/liner clearance is taken up, both horizontally and in the crown; the principle of this type of sensor involves a steel wire in contact with the rock at right angles with a displacement sensor attached to the under surface of the liner; unlike the other sensors in contact with the annular space, the reserve opening for this sensor (10 cm in diameter) is not filled in;
- one humidity/temperature sensor projecting into the annular space, 15° below the horizontal axis;
- in section 9 (Figure 10), two convergence rods to measure the liner's horizontal and vertical convergence.

In addition to these sections of instrumentation, two temperature profiles would be measured (one measuring point per section, 15° from the vertical axis and 15° above the horizontal axis) together with

the liner's overall axial strain between sections 2 and 7 (measured at the crown, 15° from the vertical axis).

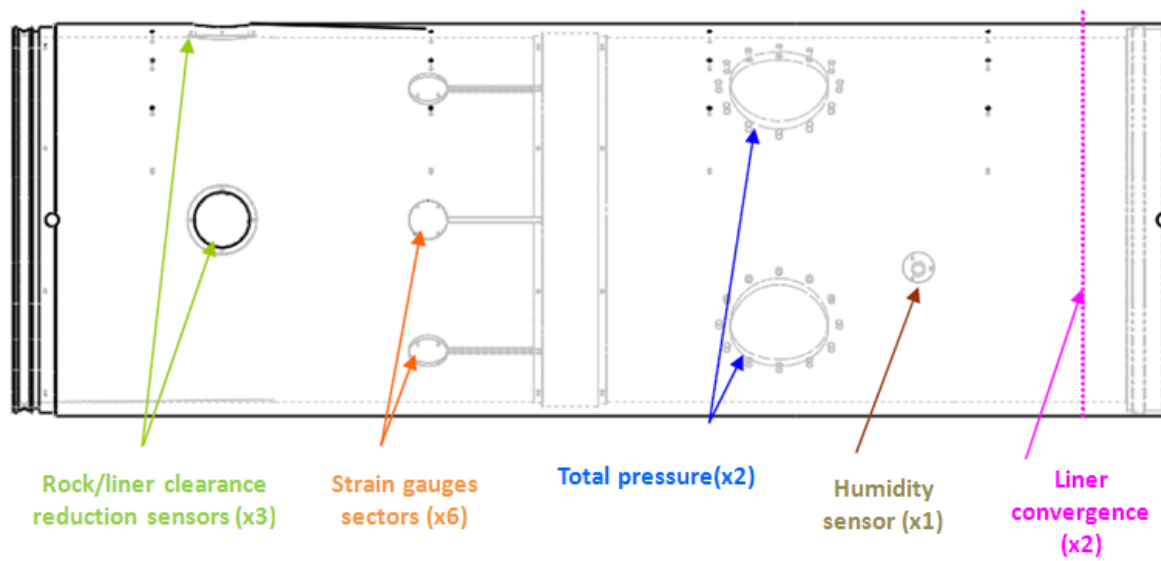
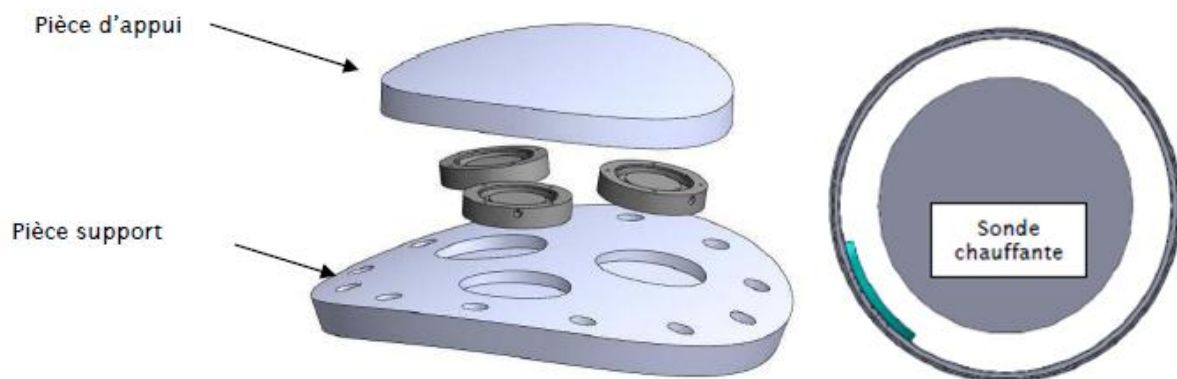


Figure 11 Locations of the sensors on the liner instrumentation sections



Figure 12 Strain gauges attached to the bottom of the spot facing on the under surface of the liner (left) – rock/liner clearance reduction sensor (right)





**Figure 13** Configuration of the total pressure sensor and position inside the cell  
(view from the end of the cell looking towards the gallery)

The two equipped insert sections each include:

- six sectors of strain gauges on the under surface, with an axial gauge and an orthoradial gauge for each sector, in the same configuration as the instrumentation on the liners;
- one humidity/temperature sensor for taking measurements in the insert, 15° below the horizontal axis;
- two convergence rods for measuring the insert's horizontal and vertical convergence.

Finally, three displacement sensors attached to the under surface of the insert and in contact with the plate at the head of the useful section, are used to measure the relative movement of the liner in the insert.

### 3.4.2 Installation sequence

Only the strain gauges were installed prior to excavation; these were positioned at the bottom of the spot facing (Figure 12) on the equipped liners and inserts and were protected by metal covers. All of the other sensors were installed, and the data cables connected, by personnel working inside the cell after the excavation phase. The cables run along the upper part of the cell in cable trays, which were installed by the personnel at the same time (Figure 14).

The installation work was completed in three phases:

- from 19 November to 12 December 2012, all of the sensors, apart from the three liner/insert relative displacement sensors, were installed and connected;
- the three convergence measurement sections of the liner (liner no. 9) and the inserts (inserts 11 and 12) were removed temporarily on 3 January 2013 to allow the heating elements to be installed in the last 15 metres of the cell (see section 3.5);
- these were replaced on 22 and 23 January 2013, when the closing plates at the head of the useful section and the head of the insert (Figure 15) and the three liner/insert relative displacement sensors were installed.



**Figure 14** *View of the three convergence measurement sections of the insert and the liner, and the cable trays*



**Figure 15** *View of the plate at the head of the useful section (left) and at the head of the insert (right)*

The closing plates, just like the end plate, were bolted onto a ring, which was itself bolted to the under surface of the liner (or insert).

Finally, only one strain gauge was not operational (on insert no. 12).

*NB: Stainless steel gas sampling lines were also installed in the cable trays along the cell: two lines running into the useful section at depths of 22 and 24 metres, and two lines leading into the insert, at depths of 2 and 5 metres.*

### **3.5 Installation of the heating elements**

The five heating elements were installed between 9 and 18 January 2013. Each heating element is 3 metres long and 508 mm in diameter, and is made up of three concentric cylinders (Figure 16):

- an empty inner cylinder, providing the space needed for the heating element cables and their instrumentation to pass through;
- an intermediate cylinder around which the two heating resistors are wound (the main resistor and the backup resistor);
- an outer cylinder used to protect the heating resistors and keep them watertight (liquid and steam phases).

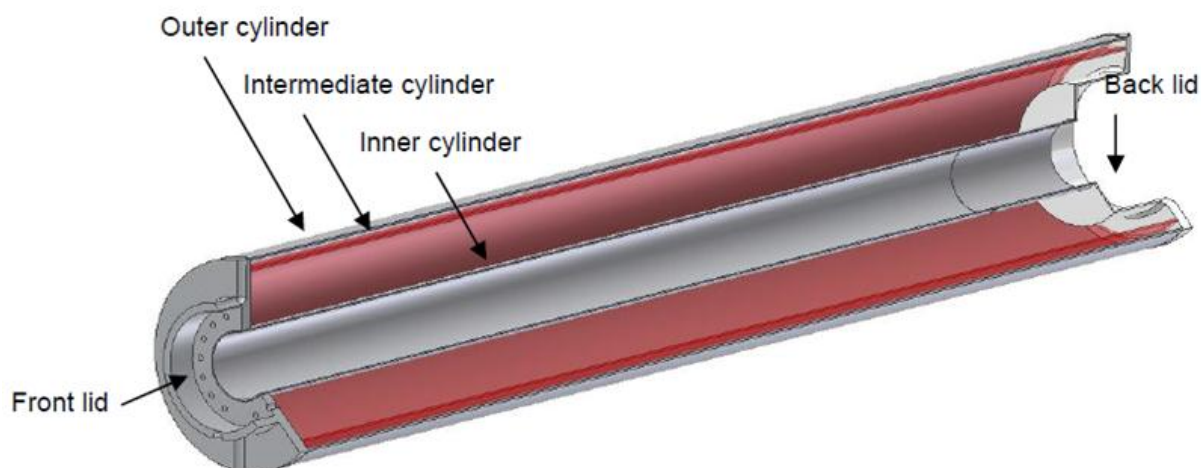


*Figure 16 Configuration of a heating element*

In addition to the temperature sensors (thermocouples) used to control the heat, each heating element contains a biaxial tiltmeter to measure any movement it might make under the effect of stress on the liner. Additionally, three liner convergence sensors, using Fabry-Perot interferometer technology, were installed at each connection between the heating elements, to take measurements on the horizontal axis and at the crown; these complete the measuring devices installed on the liner (Figure 11).

Each element has six high-resistant plastic transfer pads, fitted into metal components, which are welded to the outer cylinder (Figure 17). These pads with their small wheels made it easy to install the heating elements (each element weighs 500 kg) by running on pre-installed rails (see section 3.4). When the heating elements were inserted, the cables were passed through the inner cylinder and finally grouped together in a sleeve to pass through the closing plates (Figure 15).



*Figure 17 Installation of the heating elements – view of a section of liner convergence sensors (right)*

The control system includes one control cabinet per heating element, together with two cabinets for data acquisition and control management. The system can control both the power and the temperature. The entire system is connected to an emergency power supply to prevent any risk of a power outage during the heating phase.

### 3.6 Finalisation of the instrumentation of the cell-crossing section

Finally, the displacement sensors on the wall of the cell-crossing section were installed on 24 and 25 January 2013. These six sensors were anchored 5 cm into the concrete block (used to secure the drilling machine during the excavation) around the head of the cell. This instrumentation was completed by two connectors for the periodic manual measurement of the angle of the wall of the cell-crossing section.

A humidity/temperature sensor was also put into position at this time, just above the cell.

## 4. Initial results

This section presents the data acquired during the excavation of the cell, and describes how these data have evolved since then, including during the low-power heating test (33 W/m) conducted from 30 January to 15 February 2013, during which time the temperature reached 30°C on the liner.

### 4.1 Impact of the cell excavation

The hydro-mechanical impact of the cell excavation was monitored on the peripheral boreholes. With the exception of borehole ALC4002, whose measuring chamber was affected by sealing problems during saturation, the interstitial overpressures measured in the lateral plane to the cell for the other boreholes (ALC4001 and ALC1616) were consistent with the measurements taken during the excavation of the previous cells positioned according to the major horizontal stress (Figure 18). The time taken to reach the peak pressure increased with the distance to the wall (Figure 19), reaching 57 days for the chamber located 2.41 metres from the cell's wall (2.78 metres from the centre of the cell).

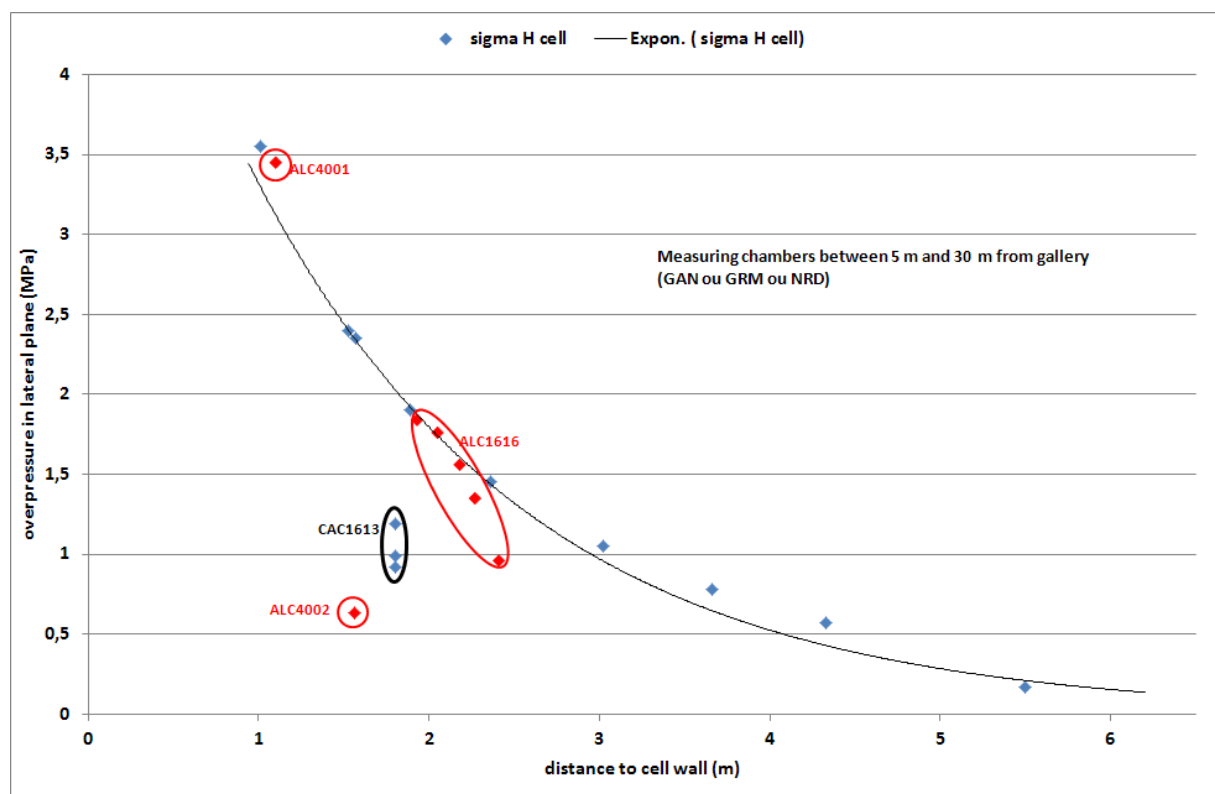


Figure 18

Overpressures measured in the lateral plane during the excavation of cells positioned according to  $\sigma_H$  – the boreholes associated with the heating cell are shown in red

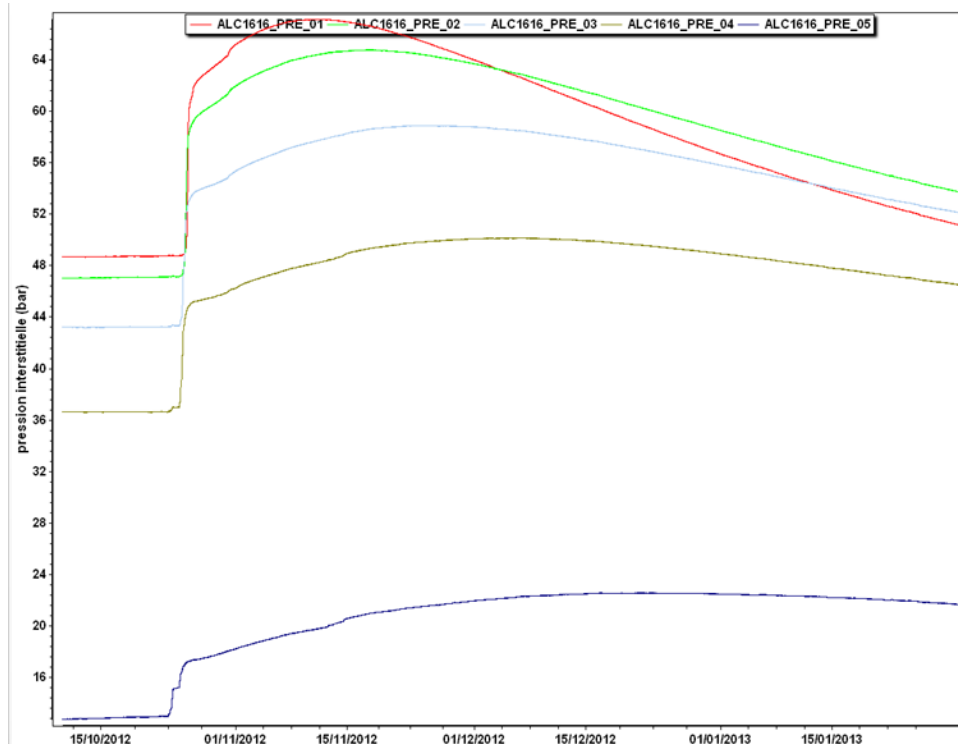


Figure 19 Pressures measured (bar) in lateral borehole ALC1616 - chambers located at 1.93, 2.05, 2.18, 2.27 and 2.41 metres from the cell's wall

In the vertical plane, the behaviour was also similar to that observed previously, with a pressure drop at the excavation face preceded by a slight overpressure (Figure 20). The measured interstitial pressure drops were found to be greater as the distance to the wall of the cell decreased (Figure 21).

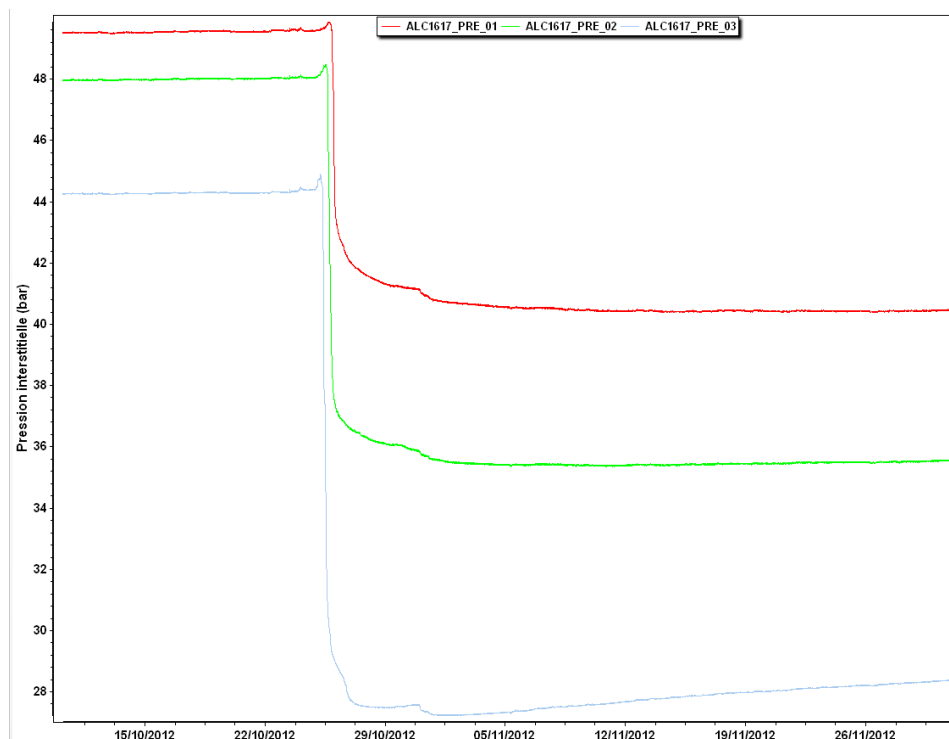


Figure 20 Pressure drops measured (bar) in the vertical plane above the cell - chambers at 2.17, 2.8 and 3.47 metres from the cell's wall



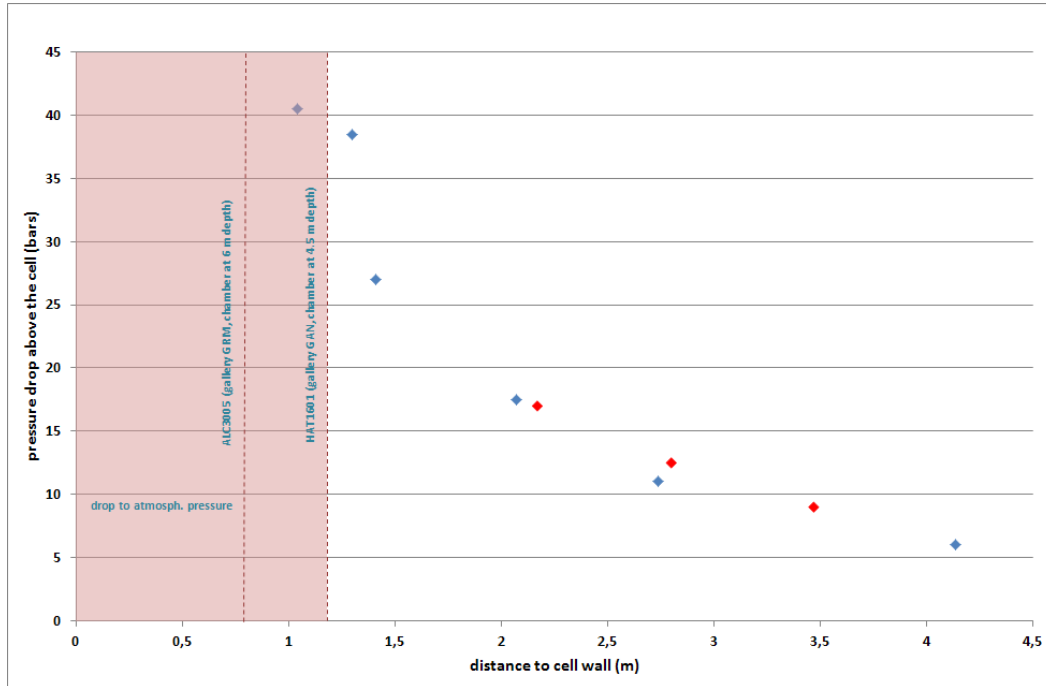


Figure 21 Pressure drop in the vertical plane (above) across the excavation face of cells positioned according to  $\sigma_H$  – the borehole associated with the heating cell (ALC1617) is shown in red

Borehole ALC4005, running perpendicular to the cell and gradually passing over it (Figure 2 and Figure 3), demonstrated an intermediate behaviour, with a drop in pressure for the measuring points located in more of a vertical plane to the cell, and an overpressure for the measuring points located more laterally (Figure 22).

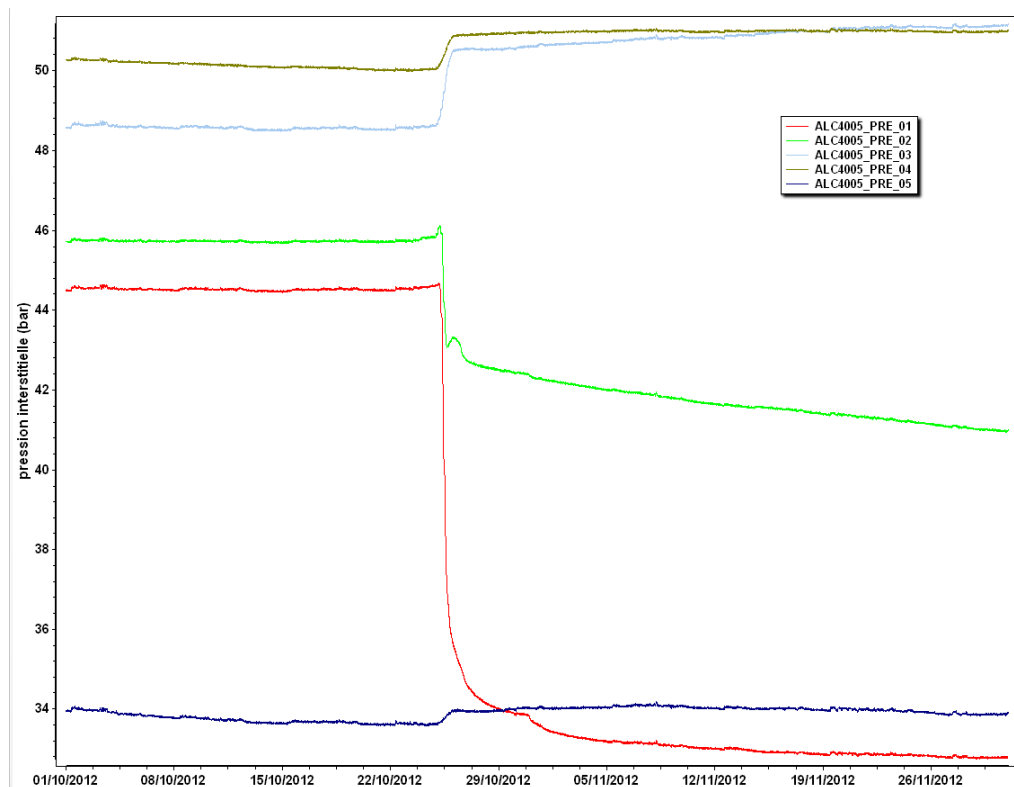
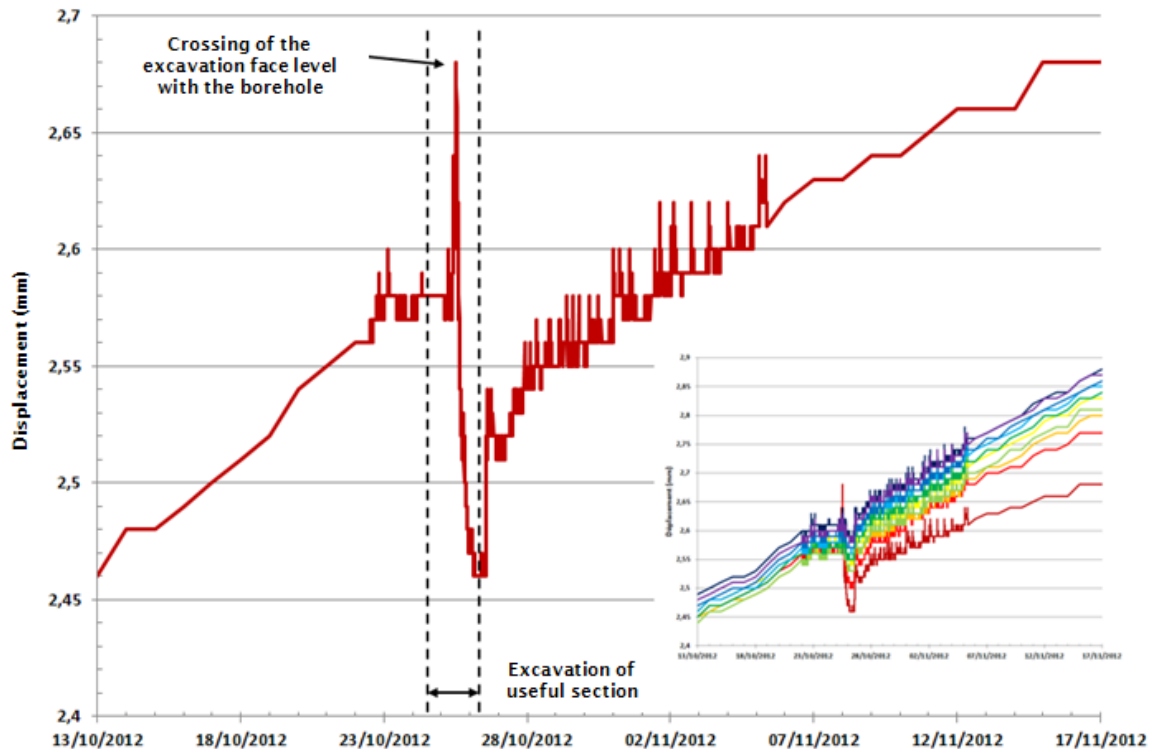


Figure 22 Changes in the interstitial pressure measured in the five chambers of borehole ALC4005

The lateral movements were also measured using the Mag-X extensometer in borehole ALC4004. Figure 23 shows the maximum movements recorded on the extensometer measuring point closest to the cell's wall, at 0.87 metres. As the excavation face came level with the extensometer borehole, this initially resulted in the convergence of the point towards the cell (extension) by 0.10 mm, followed by a compression of 0.22 mm, before a final relaxation towards the cell corresponding to de-containment (without completely returning to the initial level).



**Figure 23** *Displacements measured on the Mag-X point closest to the wall of the cell during its excavation with, inset, the same phenomenon observed on the first 10 points with a decreasing intensity according to the distance from the wall*

## 4.2 Measurements evolution in the cell

The liner instrumentation was installed between November and December 2012, as described in section 3.4.2. Data acquisition began as the sensors were installed and connected.

Measurements evolution since the sensors were connected is described in the following paragraphs, according to the instrumentation sections represented in Figure 10.

### 4.2.1 Liner and insert convergence sensors

The convergence measurement sections are located on liner no. 9, at a depth of 7 metres, and on inserts 11 and 12, at depths of 4 and 2 metres respectively in the cell.

Figure 24 shows evolution in the measurements since the sensors were connected on 13 December 2012, 48 days after the cell was excavated. It should be noted that the measurements were interrupted for 19 days from 3 to 22 January 2013, while the heating elements were being installed in the cell.

For the liner section, a convergence was observed in the horizontal direction, with an almost equivalent divergence in the vertical direction. This behaviour was similar to that observed on the previous cells positioned in the same direction, i.e. an anisotropic loading of the liner caused by a greater convergence of the rock mass in the horizontal direction. The liner was found to be under load as soon as the first measurements were taken, increasing at a rate equivalent to the values measured by the instrumentation in cell CAC1601 (Figure 25).

Conversely, the two insert sections were not subjected to any loads when the measurements began. Insert no. 11 started to experience loading after around 100 days, but with a contrasting profile to the liner, namely a convergence in the vertical direction and an equivalent divergence in the horizontal direction. This tendency needs to be verified by monitoring over a longer period and checking the corresponding sensor connections. Insert no. 12 did not show any signs of loading after almost 180 days.

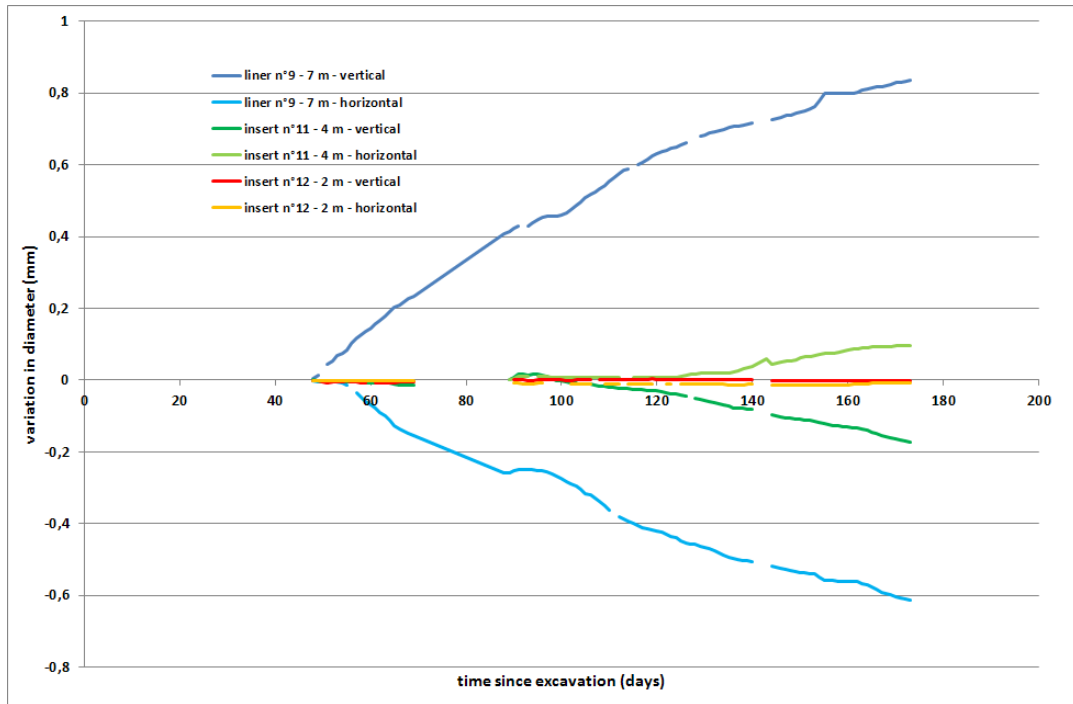


Figure 24

*Variations in diameter measured on the liner at a depth of 7 metres and on the insert at 4 and 2 metres – negative convergence, positive divergence*

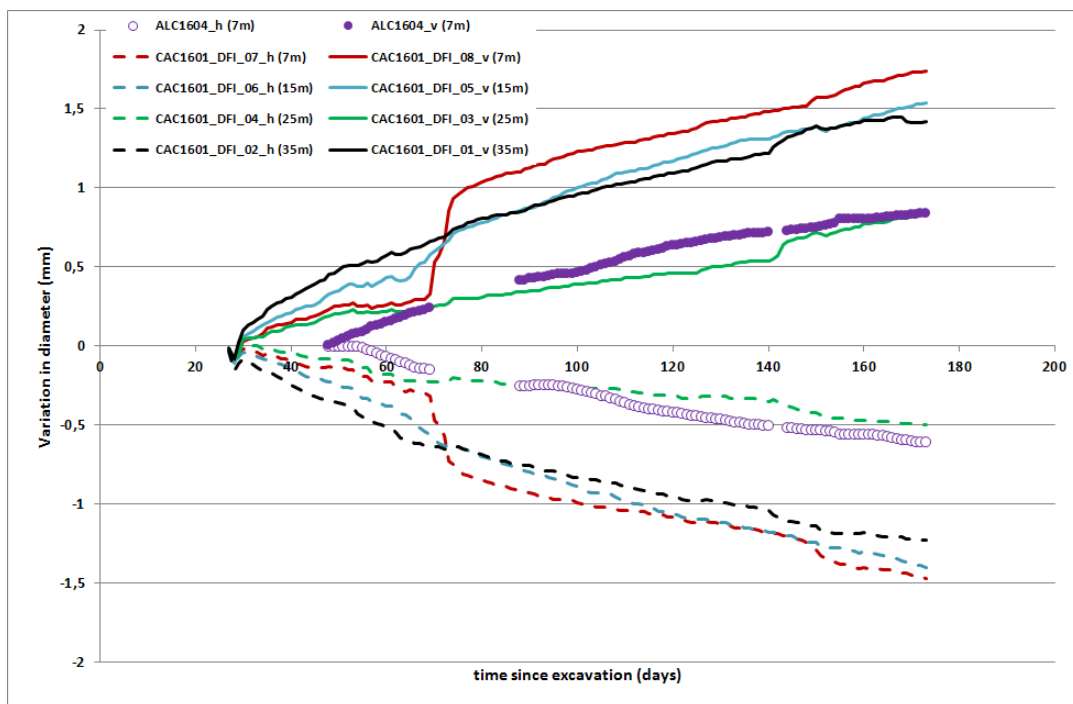


Figure 25

*Comparison between the variations in diameter measured on the liners of cells ALC1604 and CAC1601*



It is worth noting that no significant influence was observed on the variations in diameter during the low-power heating test performed between 30 January and 15 February 2013 (i.e. from the 96th to the 112th day, see section 4.3).

#### **4.2.2 Convergence sensors on the heating elements**

The heating element convergence sensors were installed at each junction between the heating elements and are used to measure the changing distances between the upper surfaces of the heating elements and the under surface of the liner, in the crown and horizontally on each side of the heating elements. The four sections of three sensors were installed at depths of 21.5, 18.5, 15.5 and 12.5 metres in the cell.

The two horizontal sensors in the deepest section (21.8 m), the vertical sensor in the 18.8 m section and a horizontal sensor in the 15.8 m section were lost during installation due to optic fibre damage.

These sensors began taking measurements on 1 February 2013, 98 days after the cell was excavated and two days after the low-power heating test started. A variation of a few tenths of a millimetre was observed on most of the sensors during the heating test, which appears to indicate that the measurements are influenced by the temperature. The measurements evolution should be monitored over a longer period, particularly during the main heating phase, so that it can be analysed more closely.

#### **4.2.3 Rock/liner clearance reduction sensors**

The sections in which the rock/liner clearances are measured are located on liners 2, 4, 6 and 9, at depths of 22.5, 18.5, 14.5 and 8.5 metres respectively in the cell.

Figure 26 shows the evolution in the measurements taken since the sensors were connected on 24 November 2012 for the sections at 22.5 and 18.5 metres, and on 5 December 2012 for the sections at 14.5 and 8.5 metres, respectively 29 and 40 days after the cell was excavated.

Some of the clearance was taken up in the crown of the cell in all four sections, varying after around 180 days between 0.33 and 0.94 mm. The movement of 0.33 mm measured at 8.5 metres was less than half of the value for the extension of the liner, in the vertical direction, measured on the same section at a depth of 7 metres (0.83 mm, see Figure 24). This variation could be explained by a difference in the cell's profile or in the overall dimensions of the annular space, due to rubble around the measuring points (even though these two measurements were taken 1.5 metres apart), involving a different load on the liner. Alternatively, it could be explained by a partial extension of the liner downwards (the diameter variation measurement was diametral whereas the clearance take-up measurement was only taken in the crown) in case the liner would not rest on the floor in this area, or by a combination of both of these factors.

The horizontal clearance take-up was more disparate across the different sections, with a diametral total varying after around 180 days between 0.15 and 1.63 mm. Some of the sensors did not register any clearance take-up, although no contact with the liner was observed when they were installed. This leads us to suppose that the rubble in the annular space around the sensors was initially stopping the clearance take-up, which could start later (after 100 days, for example, for the left sensor in the section at 18.5 metres). The total movement measured at 8.5 metres was smaller than the convergence of the liner measured horizontally on the same section at a depth of 7 metres (0.32 compared to 0.61 mm), which is consistent with contact (wall or rubble in the annular space) with the liner at the level of the convergence measurement, explaining its loading in this direction and the presence of rubble in the annular space partly blocking the clearance take-up.

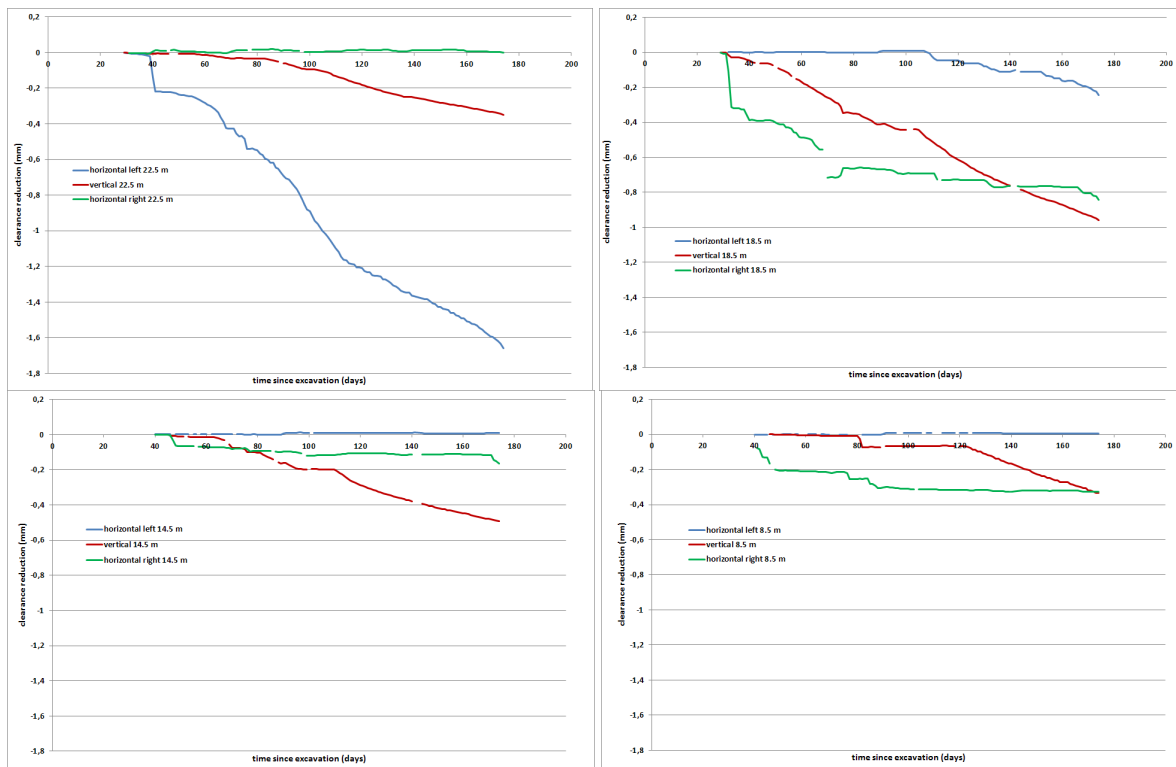


**Figure 26** *Evolution in clearance take-up between the rock and the liner at depths of 22.5, 18.5, 14.5 and 8.5 metres*

The low-power heating test between 30 January and 15 February 2013 did not appear to influence these sensors either.

#### 4.2.4 Strain gauges

The strain gauges, pre-installed on liners 2, 4, 6 and 9 and on inserts 11 and 12, at depths of 22, 18, 14, 8, 4.5 and 3 metres respectively in the cell, were connected on 22 November 2012, 27 days after the cell was excavated. Of the two gauges that were not working on that date (out of a total 72 gauges, 12 per instrumentation section), one was recovered on 23 January 2013, and the other was lost (on insert no. 12).

The strain values after around 180 days remained low, generally under 100  $\mu\text{m}/\text{m}$ . The low-power heating test only resulted in strain values of around 10 to 15  $\mu\text{m}/\text{m}$ , for an increase in temperature on the liner of 6°C.

A more detailed analysis of the strains will be conducted during the heating phase when more marked tendencies will be measured.

#### 4.2.5 Total pressure values

The total pressure sensors, installed on liners 2, 4, 6 and 9, at depths of 21.5, 17.5, 13.5 and 7.5 metres respectively in the cell, were connected between 3 and 10 December 2012, 38 to 45 days after the cell was excavated.

After around 180 days, these sensors revealed no significant variation, showing no evidence of contact between the liner and the cell wall adjacent to the sensors. This observation does not seem to be consistent with the measured diameter variations (see section 4.2.1). As for the strain values, a more detailed analysis will be conducted during the heating phase when more marked tendencies will be measured.

#### 4.2.6 Axial extensometer and liner/insert sliding sensors

The axial extensometer, installed in the crown between liner sections 2 and 7, was connected on 10 December 2012. The three liner/insert sliding sensors were connected on 23 January 2013.

These sensors, which take measurements in an axial direction to the cell, have not been influenced thus far, and did not show any significant change during the low-power heating test (no variation for the axial extensometer and around 0.1 mm for the three liner/insert sliding sensors).

#### 4.2.7 Relative humidity in the cell

The humidity/temperature sensors were installed on liner sections 2, 4, 6 and 9 and inserts 11 and 12, at depths of 21.5, 17.5, 13.5, 7.5, 4 and 2 metres respectively in the cell, and 15° below the horizontal axis. The liner sensors are used to measure the relative humidity and the temperature in the annular space between the rock and the liner; the insert sensors measure the relative humidity and the temperature in the insert. These sensors were connected on 12 and 13 December 2012.

Figure 27 shows the changes in the relative humidity over the first 180 days after excavation. In the annular space between the rock and the liner, the relative humidity quickly reached 95% (almost as soon as the first measurements were taken, around 50 days after excavation) then continued to increase slowly as observed for cell CAC1601, which was fitted with instrumentation in the same way. The sensor at 17.5 metres registered a sudden increase from 96 to 100% in a few days, which could be explained by a sensor malfunction or very localised incoming water (this phenomenon was not observed on the other sensors) leading to a sensor malfunction. In the insert, the change in the relative humidity followed the variations measured in the GAN gallery.

The low-power heating test between 30 January and 15 February 2013 (from the 96th to the 112th day after excavation) resulted in a decrease of around 5% in the relative humidity, essentially at the three measuring points located in the heated area.

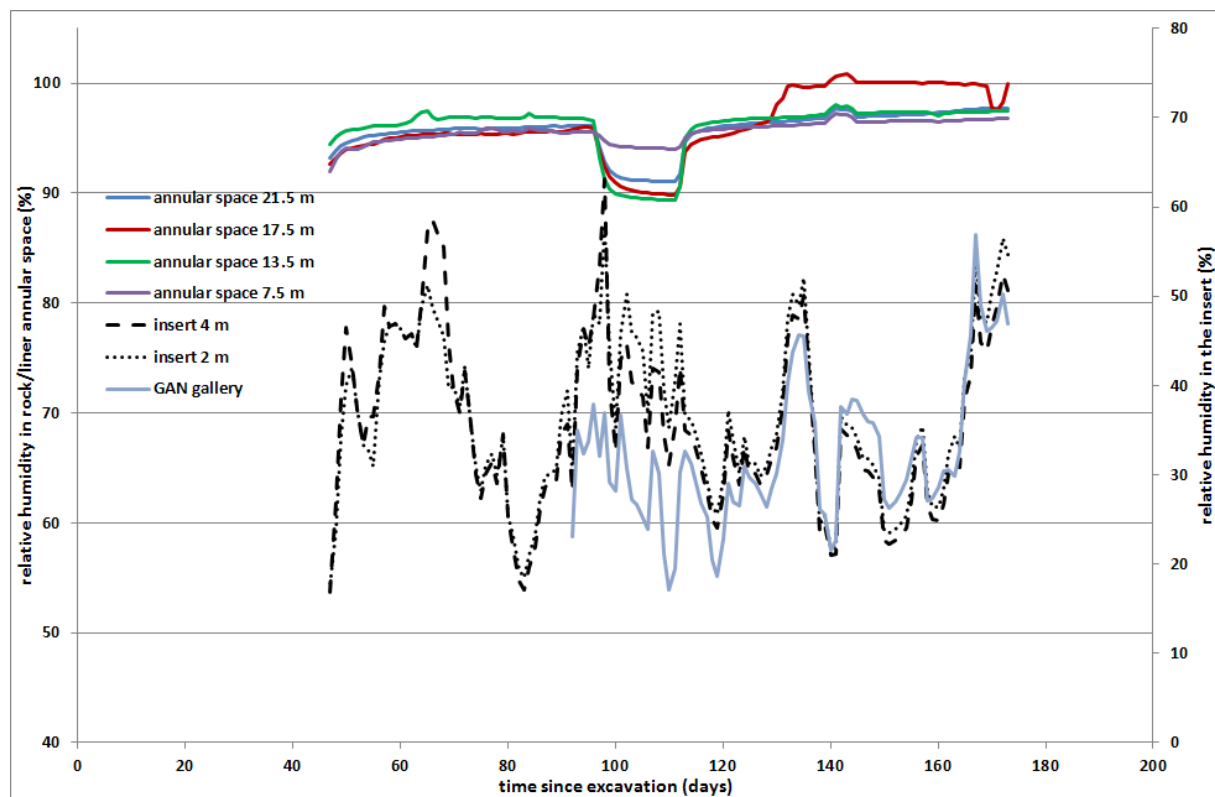


Figure 27 Evolution in the relative humidity in the heating cell - rock/liner annular space and insert, and GAN gallery

### 4.3 Low-power heating test

A low-power heating test, at 33 Watts/metre, was carried out between 30 January and 15 February 2013, to check that the heating control system and all sensors were working correctly.

#### 4.3.1 Temperature evolution inside the cell

Figure 28 shows the evolution in the two temperature profiles along the cell, 15° from the vertical axis (high profile) and 15° above the horizontal axis (low profile). The profiles consist of 13 measuring points, one point per section of liner or insert.

The temperature in the heated area reached 28 to 30°C on the liner wall (the sensor at 24 metres in the high profile appeared to malfunction). The temperature of the high profile was slightly higher than that of the low profile (however, the heating elements are theoretically very slightly off-centre, being 2 mm lower).

The temperature in the insert is influenced by the temperature in the GAN gallery, particularly on the sensor closest to the gallery.

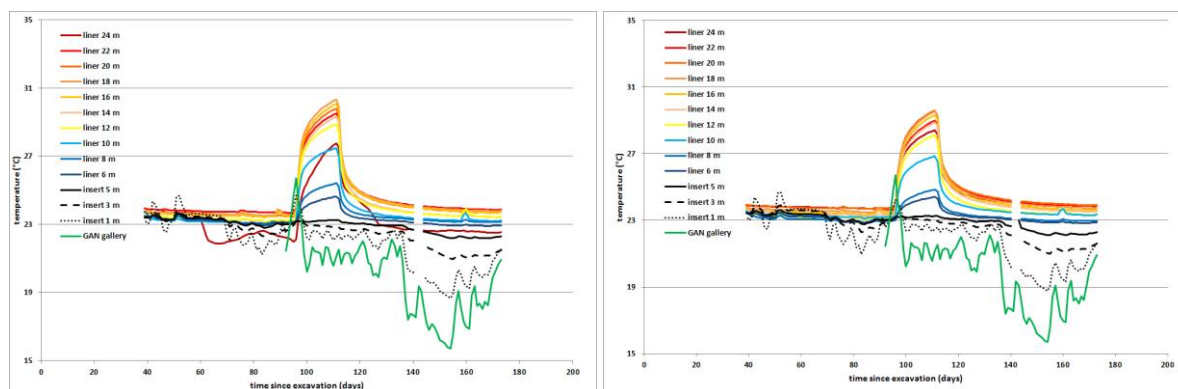


Figure 28 Evolution in the temperature on the liner and insert walls – high profile (left) and low profile (right)

#### 4.3.2 THM impact on the rock mass

The low-power heating test had a very low impact on the surrounding rock mass. For example, Figure 29 shows the evolution of the interstitial pressure and the temperature in the chamber of borehole ALC4001, closest to the cell located at 1.1 metres from the wall in the lateral plane (see Table 2 and Figure 3). The increase in temperature of 6°C on the liner wall caused an increase in the interstitial pressure of around 1 bar, for an increase in temperature in the chamber of around 1°C (which seems low in light of the feedback from the TED experiment).

The main heating phase, at 220 W/m, should allow the temperature to reach 90°C on the liner wall in around two years. This phase, launched on 18 April 2013, should see more pronounced changes, which will be analysed in more detail.

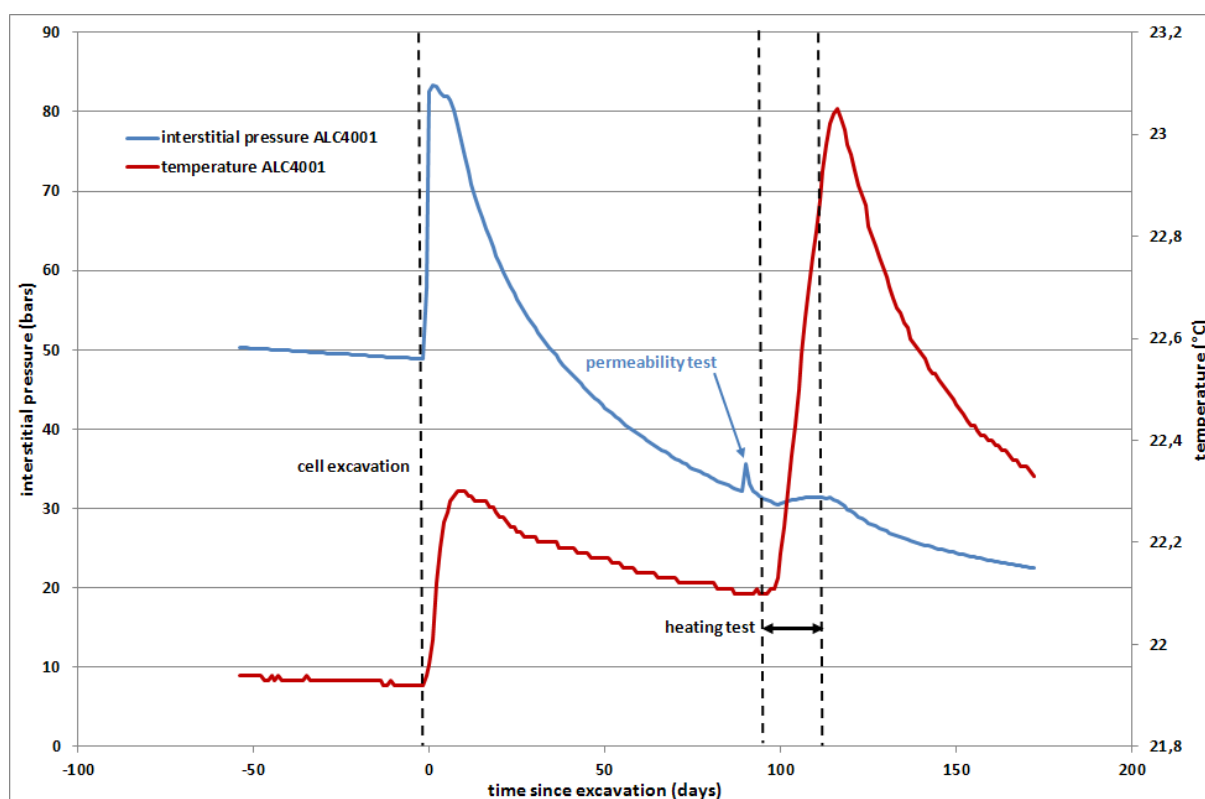


Figure 29 Evolution of the interstitial pressure and temperature in the chamber of borehole ALC4001 during the excavation of the cell and the heating test

## 5. Conclusion

The excavation of the heating cell was successfully completed, despite the drilling machine becoming blocked 70 cm from the target depth, and the final length of the cell being 24.8 metres (instead of 25 metres).

The hydro-mechanical impact of the excavation measured on the surrounding rock mass was consistent with observations made during the excavation of the previous cells positioned in the same direction in relation to the stress field.

All of the sensors installed in the cell are operational, apart from one strain gauge on the insert and four liner convergence sensors positioned on the heating elements.

The initial variations in the diameter of the liner, caused by the convergence of the cell's wall before the heating phase, were also consistent with the measurements taken in cell CAC1601 with its instrumentation, and demonstrate the loading of the liner in the horizontal direction. The insert showed that loading started at a depth of 4 metres, around 100 days after the cell was excavated, but following a contrasting profile to that observed on the liner. This behaviour will need to be checked over a longer period.

The low-power heating test (33 W/m) was performed successfully between 30 January and 15 February 2013. The main heating phase began on 18 April 2013, at 220 W/m, and will enable a temperature of 90°C to be reached on the liner wall in around two years.